J Membrane Biol (2007) 215:49–56
DOI 10.1007/s00232-007-9004-5

Developmental Expression of the Outer Hair Cell Motor Prestin in the Mouse

Takahisa Abe · Seiji Kakehata · Rei Kitani · Shin-ichiro Maruya · Dhasakumar Navaratnam · Joseph Santos-Sacchi · Hideichi Shinkawa

Received: 11 July 2006 / Accepted: 22 January 2007 / Published online: 6 April 2007

Abstract The development of motor protein activity in the lateral membrane of the mouse outer hair cell (OHC) from postnatal day 5 (P5) to P18 was investigated under whole-cell voltage clamp. Voltage-dependent, nonlinear capacitance (C_v), which represents the conformational fluctuations of the motor molecule, progressively increased during development. At P12, the onset of hearing in the mouse, C_v was about 70% of the mature level. C_v saturated at P18 when hearing shows full maturation. On the other hand, C_{lin}, which represents the membrane area of the OHC, showed a relatively small increase with development, reaching steady state at P10. This early maturation of linear capacitance is further supported by morphological estimates of surface area during development. These results, in light of recent prestin knockout experiments and our results with quantitative polymerase chain reaction, suggest that, rather than the incorporation of new motors into the lateral membrane after P10, molecular motors mature to augment nonlinear capacitance. Thus, current estimates of motor protein density based on charge movement may be exaggerated. A corresponding indicator of motor maturation, the motor's operating voltage midpoint, V_{pkcm}, tended to shift to depolarized potentials during postnatal development, although it was unstable prior to P10. However, after P14, V_{pkcm} reached a steady-state level near –67 mV, suggesting that intrinsic membrane tension or intracellular chloride, each of which can modulate V_{pkcm}, may mature at P14. These developmental data significantly alter our understanding of the cellular mechanisms that control cochlear amplification and provide a foundation for future analysis of genetic modifications of mouse auditory development.

Keywords Development · Mouse outer hair cell · Motor protein · Hearing · Cochlear amplification

T. Abe · S. Kakehata (✉) · R. Kitani · S.-i. Maruya · H. Shinkawa
Department of Otorhinolaryngology, Hirosaki University School of Medicine, Hirosaki 036-8562, Japan
e-mail: seijik@cc.hirosaki-u.ac.jp

D. Navaratnam
Department of Neurology and Neurobiology, Yale University School of Medicine, New Haven, Connecticut 06510, USA

J. Santos-Sacchi
Department of Otolaryngology and Neurobiology, Yale University School of Medicine, New Haven, Connecticut 06510, USA

Introduction

The organ of Corti, the auditory sensory epithelium of the mammal, has two types of hair cells, the inner hair cell (IHC) and the outer hair cell (OHC). In mammals, the OHC can contract and elongate at acoustic frequencies upon electrical stimulation (Brownell et al. 1985; Ashmore 1987; Santos-Sacchi 1992; Dallos and Evans 1995; Frank, Hemmert and Gummer 1999). Such voltage-depesndent length change is termed ''electromotility'' and is thought to provide a means for improving mammalian cochlear sensitivity and frequency selectivity (Dallos 1992). Recently, on the basis of subtractive cloning between motile OHCs and nonmotile IHCs, a cDNA clone that is specifically expressed in OHCs was isolated and termed ''Prestin'' (Zheng et al. 2000b). The expressed motor protein prestin, which resides exclusively in the lateral membrane (Belyantseva et al. 2000), is likely key to cochlear amplification (Zheng et al. 2000b; Liberman et al. 2002). It is common practice to evaluate OHC motor activity either by

measuring changes in OHC length or motor-derived nonlinear capacitance (C_v), both being inextricably related (Santos-Sacchi and Dilger 1988; Ashmore 1987, 1990; Santos-Sacchi 1990, 1991). GLUT5, another protein initially considered a motor candidate (Geleoc et al. 1999) that also resides within the lateral membrane, does not express nonlinear capacitance (Ludwig et al. 2001). In the OHC, then, membrane capacitance (C_m) is the sum of motor-derived capacitance and capacitance resulting from the intrinsic capacity of membrane, i.e., surface area (Santos-Sacchi and Navarrete 2002).

The onset of hearing in the mouse is approximately at postnatal day 12 (P12), and full maturation is at P18 (Ehret 1976; Steel and Bock 1980). While the mouse is currently an important model for studies on hearing and the genetics of hearing, there is no information on the development of OHC motor activity in this species. However, OHC motor development has been studied in two other species, the rat and gerbil (He, Evans and Dallos 1994; Oliver and Fakler 1999; Belyantseva et al. 2000). He et al. (1994) reported that postnatal OHCs of gerbils begin to acquire electromotile properties at P7 in the basal cochlear turn and at P8 in the apical turn, reaching adult characteristics at about P13–14. In rat OHCs, the density of motor protein matured near P11 (Oliver and Fakler 1999; Belyantseva et al. 2000); Oliver and Fakler (1999) further concluded that the increase in membrane capacitance after P11 was due to an increase in membrane area containing the same density of motor proteins. Here, we investigated the density of the motor protein in the lateral membrane of the mouse OHC during development and demonstrate that, whereas cell size of OHCs matures at P12, voltage-dependent capacitance increases continuously up to P18. We argue that this increase, in the face of fixed surface area, derives from maturation of motor activity and not from additional motor incorporation. These observations impact on basic mechanisms of motor development as well as interpretation of genetic manipulations of the motor protein prestin.

Materials and Methods

OHCs were obtained from acutely dissected organs of Corti from C57BL/6J mice. Though this strain exhibits age-related hearing loss, normal hearing persists to 2 months of age (Wu et al. 2004). Additionally, we limited our cell harvesting to low-frequency regions (middle to apical turn) that remain normal well beyond that time. The persistence of normal cochlear amplification into adulthood indicates that development occurs normally in this strain. We additionally used this strain in order to make direct comparisons with the prestin knockout results (Liberman et al. 2002). The mice were killed in accordance with the *Guidelines for Animal Experimentation*, Hirosaki University. Cochleae were dissected, and the organs of Corti were separated from the modiolus and stria vascularis. The organs were then digested with trypsin (1 mg/ml) in external solution for 10–12 min at room temperature and transferred into 35-mm plastic dishes (Falcon, Lincoln Park, NJ) with 2 ml external solution. OHCs were isolated by gentle trituration. The dish was mounted on an inverted microscope (IX71; Olympus, Tokyo, Japan).

The external solution contained (mM) 100 NaCl, 20 tetraethylammonium, 20 CsCl, 2 $CoCl_2$, 1.52 $MgCl_2$, 10 4-(2-hydroxyethyl)-1-piperazineethanesulfonic acid (HEPES) and 5 dextrose (pH 7.2), 300 mosmol • liter^{-1}, in order to block ionic conductances. The patch pipette solution contained (mM) 140 CsCl, 2 $MgCl_2$, 10 ethyleneglycoltetraacetic acid (EGTA), 10 HEPES (pH 7.2), 300 mosmol • liter^{-1} (adjusted with dextrose).

The cells were whole-cell voltage-clamped with an Axon (Burlingame, CA) 200B amplifier using patch pipettes having initial resistances of 3–5 MΩ. Series resistances, which ranged 5–20 MΩ, remained uncompensated for C_m measurements, though corrections for series resistance voltage errors were made offline. All data acquisition and analyses were performed with the Windows-based patch-clamp program jClamp (SciSoft, New Haven, Connecticut).

C_m functions were obtained 1 min after establishment of the whole-cell configuration, following sufficient time for wash-in of pipette solutions in these small cells. C_m was assessed using a continuous high-resolution (2.56 ms sampling) two-sine voltage stimulus protocol (10 mV peak at both 390.6 and 781.2 Hz) superimposed onto a voltage ramp (200 ms duration) from –150 to +150 mV (Santos-Sacchi 2004; Santos-Sacchi, Kakehata and Takahashi 1998). Capacitance data were fit to the first derivative of a two-state Boltzmann function (Santos-Sacchi 1991).

$$C_m = Q_{\max}\frac{ze}{kT}\frac{b}{(1+b)^2} + C_{lin}$$

$$b = \exp\left(\frac{-ze(V_m - V_{pkcm})}{kT}\right)$$

where $Q_{\max}$ is the maximum nonlinear charge moved, V_{pkcm} is voltage at peak capacitance or half-maximum charge transfer, V_m is membrane potential, z is valence, C_{lin} is linear membrane capacitance, e is electron charge, k is Boltzmann's constant, and T is absolute temperature. Density was calculated as $d = (Q_{max}/e)/(C_{lin}/0.008)$, i.e., based on a conversion of 0.008 pF/μm^2 (as measured directly, *see* Results). This conversion factor is within the range of factors commonly used (Solsona, Innocenti and Fernandez 1998). A further discussion of OHC linear capacitance can be found in Santos-Sacchi and Navarrete

(2002). For analyses, we quantified C_v, an estimate of voltage-dependent, nonlinear capacitance (NLC), as the absolute peak capacitance minus linear capacitance. In order to estimate surface area (A_{ohc}), we modeled the OHC as a cylinder composed of three pieces, the cuticular plate area (A_{cut}), the lateral membrane area (A_{lat}) and the basal area (A_{bas}). Cell width was determined at three equidistant positions along the cells' length.

$$A_{ohc} = A_{lat} + A_{cut} + A_{bas}$$

where

$$A_{lat} = 2\pi r(L - r)$$

$$A_{cut} = \pi r^2$$

$$A_{bas} = \frac{\pi(2r)^2}{2}$$

For P5–8 (*see* Fig. 1B), where the length and width were similar and the cell appeared more spherical, area was calculated as a sphere with an average diameter: (width + length)/2. Cell width for this age group was measured at the cell's midpoint. Dimensions were measured at 1 min following membrane patch rupture. On average, cell lengths are compressed 5.99% after the whole-cell configuration. OHC images were captured by a digital charge-coupled device camera and recorded with AQUA-Lite (version 1.2; Hamamatsu, Shizuoka, Japan). All data are given as mean ± standard error of the mean (SEM). Fits to the data were made with a sigmoidal logistic function (Sigma Plot 9.0; Systat, San Jose, California). All electrophysiological and morphometric measures were made on each cell for direct comparison.

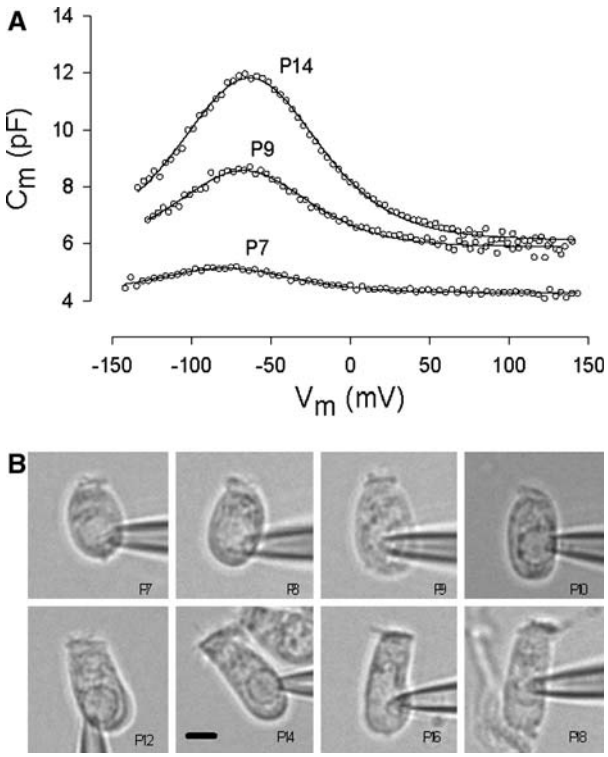

Fig. 1 (*A*) Examples of C_m functions from three postnatal days. In addition to an increase in peak capacitance, note the shift in V_{pkcm} to the right during maturation. Fitted parameters were Q_{max} = 0.091 pC, z = 0.89 at P7; Q_{max} = 0.263 pC, z = 0.95 at P9; Q_{max} = 0.542 pC, z = 0.89 at P14. (*B*) Images of patch-clamped OHCs from P7 to P18. Scale bar (7.5 μm) in P14 figure applies to all images

To estimate the prestin mRNA level during development, a two-step reverse transcription (RT) and quantitative polymerase chain reaction (QPCR) was employed. Total RNA was extracted from the organ of Corti at P5, P8, P10 and P15, using TRI reagent and reverse-transcribed using random decamers according to the manufacturer's instructions (Invitrogen, Carlsbad, CA). QPCR was done using a 1:10 dilution of cDNA. QPCR was performed with a Brilliant SYBR Green qPCR kit and Stratagene MX3000 (both from Stratagene, La Jolla, CA). Each amplification was done in duplicate. Amplification conditions were 94°C for 30 s, 60°C for 30 s and 72°C for 1 min. Primer sequences were as follows: prestin, TGGGGTCAAAACAAAGCGG and GCAAACCAAAAACCATCAGGC (spanning intron between exons 8 and 9); glyceraldehyde-3-phosphate dehydrogenase (GAPDH), AGGTCGGTGTGAACGGATTTG and TGTAGACCATGTAGTTGAGGTCA. Amplification specificity was confirmed by melting curve analysis and agarose gel electrophoresis (Metaphor; ICN, Irvine, CA). Data were normalized to GAPDH expression.

Results

The signature electrical response of an adult OHC is a bell-shaped, voltage-dependent capacitance. In postnatal OHCs, C_m showed bell-shaped voltage dependence from P7; C_v was not detectable at either P5 or P6. Examples of the change of C_m functions with development are shown in Figure 1A. Examples of digitally captured phase-contrast images of developing OHCs are shown in Figure 1B. From such data we determined estimates of the cells' linear capacitance (a correlate of membrane surface area), which increased slightly from P5 to P9, thereafter remaining stable (Fig. 2A, colored symbols). In that same figure, surface area estimates (see Materials and Methods) correspond to measures of C_{lin}. Linear capacitance measures more accurately assess the surface area since these measures are not dependent on geometrical models. Although surface area remains fixed after P9, dimensions change, with cell width decreasing and cell length increasing. A plot of their correspondence (Fig. 2B) shows this inverse relationship and indicates that after OHCs attain about

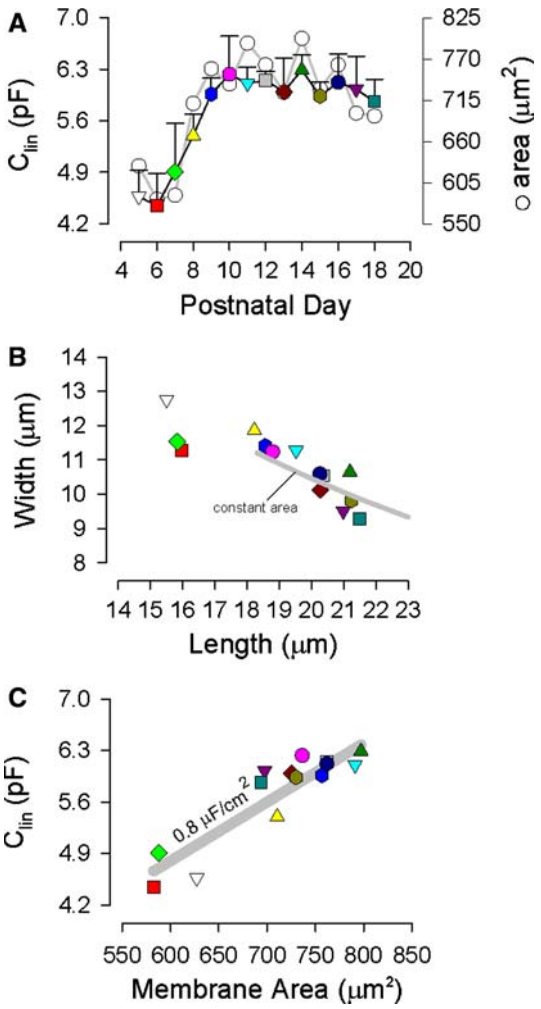

Fig. 2 Cell dimensions as a function of postnatal day. (*A*) Linear capacitance (with standard error bars) and surface area as a function of postnatal day. Note saturation of each measure at P10. (*B*) Inverse relationship between measured length and width of OHCs. *Solid gray line* denotes constant surface area constraint on width *vs.* length for the cylindrical model (see Materials and Methods). Surface area was constrained at 740 μm^2 (P10). (*C*) Relationship between linear capacitance and calculated surface area. *Solid gray line* denotes a specific membrane capacitance of 0.008 $pF/\mu m^2$

18 μm in length, dimensional changes are constrained by constant surface area (solid gray line). That is, length and width of the cylindrical cell continue to change during development but do so while maintaining a fixed surface area. A specific membrane capacitance of 0.008 $pF/\mu m^2$ characterizes the plasma membrane of developing OHCs (Fig. 2C).

NLC, unlike linear capacitance, increases throughout the developmental time period studied. Figure 3A shows the sigmoidal rise of C_v (colored symbols), reaching a saturating level (7.66 pF) at P18. Correspondingly, the unitary charge density (open circles) increases to saturation (10,956 $e^-/\mu m^2$) but, being determined by the surface area (which remains fixed above P9), shows a relative boost, over C_v, as maturation advances. The bimodal change in C_v *vs.* C_{lin} is highlighted in Figure 3B, where both C_v and C_{lin} increase linearly between P5 and P10 but, following that, only C_v increases. The changes in capacitance that occur early (P6–P10) are accompanied by a highly variable operating voltage range (V_{pkcm}, Fig. 4); however, when C_v is solely on the rise (>P10), V_{pkcm} shifts rightward to more stably occupy a voltage near –67 m*V*. The voltage sensitivity or valence, *z*, remained stable from P6 to P18 (0.875 ± 0.014).

Figure 5 shows the expression of prestin and GAPDH using a two-step RT-QPCR. Both the absolute and normalized levels of prestin RNA peaked near P10, consistent with our electrophysiological results. Absolute prestin RNA levels at P5, P8 and P15 were, respectively, 18%, 32% and 58% of that at P10. Similarly, prestin RNA levels at P5, P8 and P15, normalized to GAPDH RNA expression, were, respectively, 66%, 66% and 30% of that at P10. These quantitative data wholly support our electrophysiological conclusions that prestin expression matures at P10.

Discussion

Hearing in altricial mammals develops following birth. The mouse is first capable of detecting sounds as early as P12 (Ehret 1976; Steel and Bock 1980). However, this rudimentary ability does not benefit from the enhanced fine tuning and sensitivity afforded by cochlear amplification, the result of active, electromechanical feedback into the basilar membrane by mature OHCs. During the next several days, sensitivity and frequency tuning mature until at P18 the hearing organ is fully mature as measured by masked auditory brainstem response tuning curves (Song, McGee and Walsh 2006). Here, we provide the first detailed developmental study of mouse OHC motor protein expression in order to assess the OHCs' contribution toward the development of cochlear amplification (Zheng et al. 2000a; Liberman et al. 2002). Our data bear not only on this developing contribution toward mature audition but also on molecular mechanisms of motor maturation itself.

OHC Maturation

Certain characteristics of mouse OHC maturation correlate well with the development of hearing, though it should be kept in mind that the attainment of adult cochlear function undoubtedly profits from a concerted developmental contribution from a variety of cellular and acellular structures (Shnerson, Devigne and Pujol 1981; Shnerson and Pujol 1981; Souter and Forge 1998; Forge, Souter and Denman Johnson 1997; Souter, Nevill and Forge 1995). Nevertheless, considering the unusually important contribution of

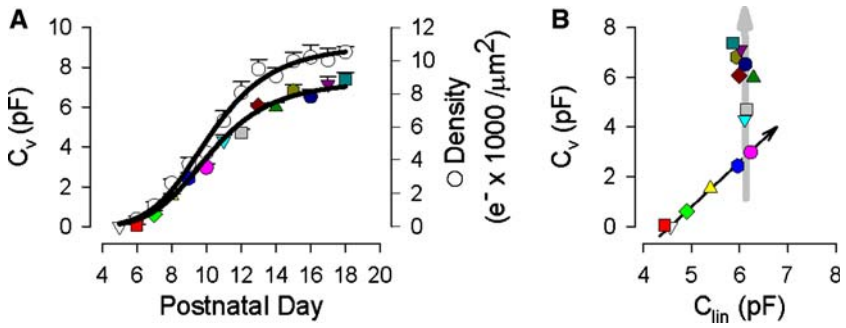

Fig. 3 (*A*) NLC (C_v, *colored symbols*) and unitary charge density (*open circles*) as a function of postnatal day. Each function saturates at P18. Charge density was computed using C_{lin} to calculate surface area with the specific membrane capacitance of 0.008 pF/μm^2. Logistic fits were made with C_v or density = max/[1+(day/mid) × b]. Charge density fit (max, b, mid): 10,956, –5.65, 10.22. C_v: 7.66, –5.33, 10.66. The number of cells was (from P5 to P18) 2, 5, 5, 9, 5, 6, 10, 9, 5, 10, 6, 9, 5 and 5. Standard error is plotted. (*B*) Relationship between C_v and C_{lin}. Note the continued increase in C_v after C_{lin} (or surface area) saturates

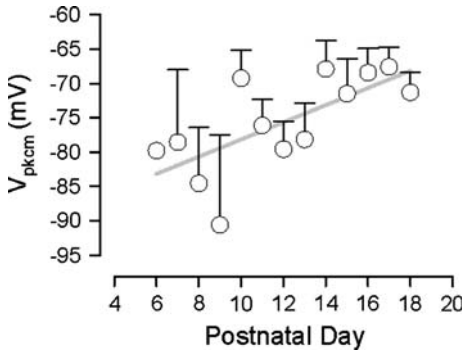

Fig. 4 Voltage at peak capacitance (V_{pkcm}) changes during development. Note variability during early stages and eventual shift toward depolarized voltages, stabilizing near –67 m*V*

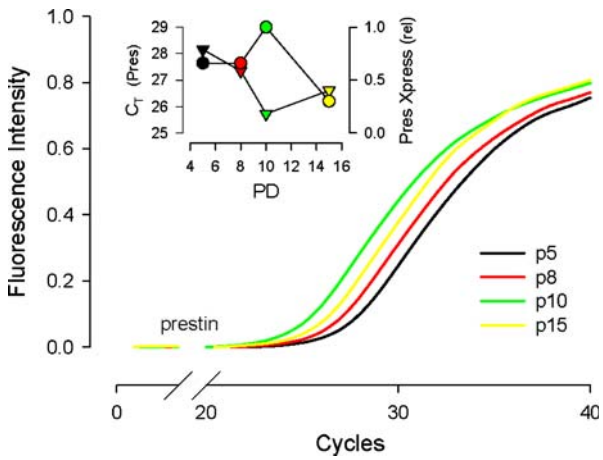

Fig. 5 Expression of prestin changes with development and peaks at P10. QPCR amplification of cDNA from cochlea RNA obtained on P5 (*black*), P8 (*red*), P10 (*green*) and P15 (*yellow*) are shown. *Inset* shows the C_t values of prestin and the relative amplification of prestin corrected for GAPDH expression at P5, P8, P10 and P15. The lower C_t value (*triangles*) at P10 confirms the highest expression at this time point. The relative expression (*circles*) of prestin is compared to expression at P10

OHCs to cochlear amplification, the development of OHC electromotility is considered one of the key features in this process. Our data show that motor activity (C_v or NLC) of the mouse OHC reaches adult levels at P18, having its onset at P7. Marcotti and Kros (1999) studied OHC motility and capacitance. However, they measured capacitance only at a fixed membrane voltage of –84 m*V*; therefore, they could not detect linear and nonlinear capacitance. In addition, they did not study beyond P12. Similar results have been found in other altricial species, including the gerbil, guinea pig and rat (Pujol et al. 1991; He et al. 1994; Oliver and Fakler 1999; Belyantseva et al. 2000). In the rat, NLC matures at P17 (Belyantseva et al. 2000) and is detectable as early as P0 in apical turn OHCs (Oliver and Fakler 1999). Interestingly, for apical turn OHCs, Oliver and Fakler (1999) found a growth correspondence in linear capacitance and NLC for P10–14, which differs from our measures that show saturation of linear capacitance in the face of increasing NLC. Consequently, we find an increasing charge density out to adult performance times (P18, Fig. 3A), whereas they calculate a saturated charge density after P11. While species differences must be considered, methodological differences in measuring NLC may play a role. Our methodology provides unbiased estimates of C_m in the face of changing voltage-dependent impedance (Santos-Sacchi 2004); however, the stair-step protocol employed by Oliver and Fakler (1999) could have been influenced by the inability of the fixed (5 ms) voltage step protocol to adequately evaluate charge transfer across the range of OHC voltage-dependent time constants evoked by the wide-ranging voltage ramp. Their early developmental data for linear capacitance (P0–10) show a saturating increase from P0, which is stable from P4 to P11. Thus, we speculate that the abrupt increase in linear capacitance that they found after P11 obscures a continuing increase in charge density out to later days.

Supporting this contention, Belyantseva et al. (2000) found nonlinear charge density to increase beyond P17 in the rat, and He et al. (1994) found an inverse relationship between length and width of developing gerbil OHCs, similar to what we found. We should also note that the developmental shift of V_{pkcm} that we observed, though similar in direction to that observed by Oliver and Fakler (1999), matured at a potential more negative than their value, i.e., near –67 m*V*, the resting potential found in adult guinea pig OHCs *in vivo* (Dallos, Santos-Sacchi and Flock 1982).

OHC Motor Maturation

Though we find that OHC motor activity saturates at P18, which is coincident with the attainment of mature hearing in the mouse, our data actually indicate that this saturation does not directly reflect the attainment of adult motor density in the lateral membrane. Instead, our data likely characterize the maturation of an already fixed pool of membrane motor proteins at P10 that we have measured with QPCR. Indeed, prestin expression in the rat has also been shown to plateau after P10 in the rat, confirming our results (Reisinger et al. 2005). These direct measures are additionally supported by the observation that motor protein membrane residence contributes to membrane surface area in the OHC. In fact, not only does prestin occupy space in the OHC membrane but the amount of surface area it occupies is voltage-dependent (Kalinec et al. 1992; Iwasa 1994; Santos-Sacchi 1993; Santos-Sacchi and Navarrete 2002). Thus, in prestin knockout mice, it was shown that the length of OHCs diminished relative to the length of normal OHCs in the control C57BL/6J mouse (Liberman et al. 2002). From Liberman et al.'s morphometric data on OHCs isolated from the apical region of the cochlea, the length reduction corresponds to about 134 μm^2 surface area occupancy by prestin. Our data show that from P6 to P10 surface area increases by about 165 μm^2, remaining fixed thereafter (Fig. 2A). This increase in surface area is coterminous with the increase in C_v that accompanies prestin expression; thus, we hypothesize that from P6 to P10 a full complement of motor proteins is expressed in mouse OHCs. Our hypothesis is strongly supported by our and others' (Reisinger et al. 2005) QPCR data, which show prestin expression to plateau at p10. Previous studies have concluded that the saturation of motor activity in the OHC represents the attainment of adult levels of motor protein density in the lateral membrane. For example, Belyantseva et al. (2000) found a correlated development of motor charge density and prestin antibody fluorescence in the lateral membrane. Souter et al. (1995) also found that the density of intramembranous particles (a presumed ultrastructural correlate of the motors) in the lateral membrane matures at P16 in the gerbil. How could the density of motors increase in the lateral membrane given our observation that a fixed pool of motors resides within the OHC following P10? In tackling this question, it must be realized that all motor charge data arise from measures of the whole OHC membrane. Recently, it has been shown that during development of rat OHCs prestin is initially expressed throughout the basolateral membrane and subsequently redistributes only to the lateral membrane between days P7 and P12 (Weber et al. 2002). Thus, it is possible for the density of motors in the lateral membrane to increase over time by redistribution into the lateral membrane, where, in the adult, motor activity is restricted (Kalinec et al. 1992; Huang and Santos-Sacchi 1993a). However, it is not clear that a simple redistribution of motors within the membrane would have an effect on the magnitude of motor charge movement. So, in the face of a fixed pool of motors following P10, how might C_v increase? It is well established that prestin-derived NLC can be modulated by a variety of biophysical forces, perhaps these forces themselves being developmentally regulated.

Two of the most significant biophysical influences on the OHC motor are its sensitivity to membrane tension and chloride ions (Iwasa 1993; Gale and Ashmore 1994; Kakehata and Santos-Sacchi 1995; Oliver et al. 2001; Rybalchenko and Santos-Sacchi 2003; Song, Seeger and Santos-Sacchi 2005), each capable of shifting V_{pkcm} and modulating the magnitude of C_v. The simultaneous changes in V_{pkcm} and C_v that we find during maturation at P10–18 may thus result from developmental changes in membrane tension and/or intracellular chloride activity. It is well known that changes in intracellular chloride levels during development can alter the anion's equilibrium potential, bringing about significant changes in inhibitory neurotransmitter response characteristics (Rivera et al. 1999). In the OHC, development of the adult architecture of the lateral wall, including the cortical cytoskeleton and its interaction with the lateral membrane, could alter membrane tension. Additionally, the increasing density of motors could alter motor-motor interactions, leading to the maturation of motor-derived tension within the membrane. Such motor interactions have been modeled to account for prepulse effects on NLC V_{pkcm} within the OHC lateral membrane and prestin transfected cells (Santos-Sacchi et al. 1998, 2001). Finally, it may be that other factors can influence the maturation of motor activity, including second messenger/phosphorylation effects on the motor itself or on associated cytoskeletal elements (Huang and Santos-Sacchi 1993b; Frolenkov et al. 2000; Deak et al. 2005).

Acknowledgement This work was supported by Grants-in-Aid for Scientific Research from the Ministry of Education, Culture, Sports, Science and Technology of Japan (to S. K., H. S.), NIH grants DC00273 (to J. S.-S.) and K08 DC05352 (to D. N.).

References

Ashmore JF (1987) A fast motile response in guinea-pig outer hair cells: The cellular basis of the cochlear amplifier. J Physiol 388:323–347

Ashmore JF (1990) Forward and reverse transduction in the mammalian cochlea. Neurosci Res Suppl 12:S39–S50

Belyantseva IA, Adler HJ, Curi R, Frolenkov GI, Kachar B (2000) Expression and localization of prestin and the sugar transporter GLUT-5 during development of electromotility in cochlear outer hair cells. J Neurosci 20:RC116

Brownell WE, Bader CR, Bertrand D, de Ribaupierre Y (1985) Evoked mechanical responses of isolated cochlear outer hair cells. Science 227:194–196

Dallos P (1992) The active cochlea. J Neurosci 12:4575–4585

Dallos P, Evans BN (1995) High-frequency motility of outer hair cells and the cochlear amplifier. Science 267:2006–2009

Dallos P, Santos-Sacchi J, Flock A (1982) Intracellular recordings from cochlear outer hair cells. Science 218:582–584

Deak L, Zheng J, Orem A, Du GG, Aguinaga S, Matsuda K, Dallos P (2005) Effects of cyclic nucleoticles on the function of prestin. J Physiol 563:483–496

Ehret G (1976) Development of absolute auditory thresholds in the house mouse (*Mus musculus*). J Am Audiol Soc 1:179–184

Forge A, Souter M, Denman Johnson K (1997) Structural development of sensory cells in the ear. Semin Cell Dev Biol 8:225–237

Frank G, Hemmert W, Gummer AW (1999) Limiting dynamics of high-frequency electromechanical transduction of outer hair cells. Proc Natl Acad Sci USA 96:4420–4425

Frolenkov GI, Mammano F, Belyantseva IA, Coling D, Kachar B (2000) Two distinct Ca^{2+}-dependent signaling pathways regulate the motor output of cochlear outer hair cells. J Neurosci 20:5940–5948

Gale JE, Ashmore JF (1994) Charge displacement induced by rapid stretch in the basolateral membrane of the guinea-pig outer hair cell. Proc R Soc Lond B Biol Sci 255:243–249

Geleoc GS, Casalotti SO, Forge A, Ashmore JF (1999) A sugar transporter as a candidate for the outer hair cell motor. Nat Neurosci 2:713–719

He DZ, Evans BN, Dallos P (1994) First appearance and development of electromotility in neonatal gerbil outer hair cells. Hear Res 78:77–90

Huang G, Santos-Sacchi J (1993a) Mapping the distribution of the outer hair cell motility voltage sensor by electrical amputation. Biophys J 65:2228–2236

Huang G-J, Santos-Sacchi J (1993b) Metabolic control of OHC function: Phosphorylation and dephosphorylation agents shift the voltage dependence of motility related capacitance. Assoc Res Otolaryngol Abs 16:464

Iwasa KH (1993) Effect of stress on the membrane capacitance of the auditory outer hair cell. Biophys J 65:492–498

Iwasa KH (1994) A membrane motor model for the fast motility of the outer hair cell. J Acoust Soc Am 96:2216–2224

Kakehata S, Santos-Sacchi J (1995) Membrane tension directly shifts voltage dependence of outer hair cell motility and associated gating charge. Biophys J 68:2190–2197

Kalinec F, Holley MC, Iwasa KH, Lim DJ, Kachar B (1992) A membrane-based force generation mechanism in auditory sensory cells. Proc Natl Acad Sci USA 89:8671–8675

Liberman MC, Gao J, He DZ, Wu X, Jia S, Zuo J (2002) Prestin is required for electromotility of the outer hair cell and for the cochlear amplifier. Nature 419:300–304

Ludwig J, Oliver D, Frank G, Klocker N, Gummer AW, Fakler B (2001) Reciprocal electromechanical properties of rat prestin: The motor molecule from rat outer hair cells. Proc Natl Acad Sci USA 98:4178–4183

Marcotti W, Kros CJ (1999) Developmental expression of the potassium current Ik, n contributes to maturation of mouse outer hair cells. J Physiol 520:653–660

Oliver D, Fakler B (1999) Expression density and functional characteristics of the outer hair cell motor protein are regulated during postnatal development in rat. J Physiol 519(pt 3):791–800

Oliver D, He DZ, Klocker N, Ludwig J, Schulte U, Waldegger S, Ruppersberg JP, Dallos P, Fakler B (2001) Intracellular anions as the voltage sensor of prestin, the outer hair cell motor protein. Science 292:2340–2343

Pujol R, Zajic G, Dulon D, Raphael Y, Altschuler RA, Schacht J (1991) First appearance and development of motile properties in outer hair cells isolated from guinea-pig cochlea. Hear Res 57:129–141

Reisinger E, Zimmermann U, Knipper M, Ludwig J, Klocker N, Fakler B, Oliver D (2005) Cod106, a novel synaptic protein expressed in sensory hair cells of the inner ear and in CNS neurons. Mol Cell Neurosci 28:106–117

Rivera C, Voipio J, Payne JA, Ruusuvuori E, Lahtinen H, Lamsa K, Pirvola U, Saarma M, Kaila K (1999) The K^+/Cl^- co-transporter KCC2 renders GABA hyperpolarizing during neuronal maturation. Nature 397:251–255

Rybalchenko V, Santos-Sacchi J (2003) Cl^- flux through a non-selective, stretch-sensitive conductance influences the outer hair cell motor of the guinea-pig. J Physiol 547:873–891

Santos-Sacchi J (1990) Fast outer hair cell motility: How fast is fast? In: Dallos P, Geisler CD, Matthews JW, Ruggero MA, Steele CR, editors. The Mechanics and Biophysics of Hearing. Springer-Verlag, Berlin, pp. 69–75

Santos-Sacchi J (1991) Reversible inhibition of voltage-dependent outer hair cell motility and capacitance. J Neurosci 11:3096–3110

Santos-Sacchi J (1992) On the frequency limit and phase of outer hair cell motility: Effects of the membrane filter. J Neurosci 12:1906–1916

Santos-Sacchi J (1993) Harmonics of outer hair cell motility. Biophys J 65:2217–2227

Santos-Sacchi J (2004) Determination of cell capacitance using the exact empirical solution of dY/dCm and its phase angle. Biophys J 87:714–727

Santos-Sacchi J, Dilger JP (1988) Whole cell currents and mechanical responses of isolated outer hair cells. Hear Res 35:143–150

Santos-Sacchi J, Kakehata S, Takahashi S (1998) Effects of membrane potential on the voltage dependence of motility-related charge in outer hair cells of the guinea-pig. J Physiol 510(pt 1):225–235

Santos-Sacchi J, Navarrete E (2002) Voltage-dependent changes in specific membrane capacitance caused by prestin, the outer hair cell lateral membrane motor. Pfluegers Arch 444:99–106

Santos-Sacchi J, Shen WX, Zheng J, Dallos P (2001) Effects of membrane potential and tension on prestin, the outer hair cell lateral membrane motor protein. J Physiol 531:661–666

Shnerson A, Devigne C, Pujol R (1981) Age-related changes in the C57BL/6J mouse cochlea. II. Ultrastructural findings. Brain Res 254:77–88

Shnerson A, Pujol R (1981) Age-related changes in the C57BL/6J mouse cochlea. I. Physiological findings. Brain Res 254:65–75

Solsona C, Innocenti B, Fernandez JM (1998) Regulation of exocytotic fusion by cell inflation. Biophys J 74:1061–1073

Song L, McGee J, Walsh EJ (2006) Frequency- and level-dependent changes in auditory brainstem responses (ABRs) in developing mice. J Acoust Soc Am 119:2242–2257

Song L, Seeger A, Santos-Sacchi J (2005) On membrane motor activity and chloride flux in the outer hair cell: Lessons learned

from the environmental toxin tributyltin. Biophys J 88:2350–2362

Souter M, Forge A (1998) Intercellular junctional maturation in the stria vascularis: Possible association with onset and rise of endocochlear potential. Hear Res 119:81–95

Souter M, Nevill G, Forge A (1995) Postnatal development of membrane specialisations of gerbil outer hair cells. Hear Res 91:43–62

Steel KP, Bock GR (1980) The nature of inherited deafness in deafness mice. Nature 288:159–161

Weber T, Zimmermann U, Winter H, Mack A, Kopschall I, Rohbock K, Zenner HP, Knipper M (2002) Thyroid hormone is a critical determinant for the regulation of the cochlear motor protein prestin. Proc Natl Acad Sci USA 99:2901–2906

Wu X, Gao J, Guo Y, Zuo J (2004) Hearing threshold elevation precedes hair-cell loss in prestin knockout mice. Brain Res Mol Brain Res 126:30–37

Zheng J, Shen W, He D, Long K, Madison L, Dallos P (2000a) Prestin is the motor protein of cochlear outer hair cells. Nature 405:149–155

Zheng J, Shen W, He DZ, Long KB, Madison LD, Dallos P (2000b) Prestin is the motor protein of cochlear outer hair cells. Nature 405:149–155